Emergent Conformal Boundaries from Finite-Entanglement Scaling in Matrix Product States

Rui-Zhen Huang,[1,*] Long Zhang,[2] Andreas M. Läuchli,[3,4] Jutho Haegeman,[1]
Frank Verstraete,[5,1] and Laurens Vanderstraeten[6]

[1]*Department of Physics and Astronomy, University of Ghent, 9000 Ghent, Belgium*
[2]*Kavli Institute for Theoretical Sciences and CAS Center for Excellence in Topological Quantum Computation, University of Chinese Academy of Sciences, Beijing 100190, China*
[3]*Laboratory for Theoretical and Computational Physics, Paul Scherrer Institute, 5232 Villigen, Switzerland*
[4]*Institute of Physics, École Polytechnique Fédérale de Lausanne (EPFL), 1015 Lausanne, Switzerland*
[5]*Department of Applied Mathematics and Theoretical Physics, University of Cambridge, Cambridge, United Kingdom*
[6]*Center for Nonlinear Phenomena and Complex Systems, Université Libre de Bruxelles, Brussels, Belgium*

(Received 3 July 2023; accepted 23 January 2024; published 23 February 2024)

The use of finite entanglement scaling with matrix product states (MPS) has become a crucial tool for studying one-dimensional critical lattice theories, especially those with emergent conformal symmetry. We argue that finite entanglement introduces a relevant deformation in the critical theory. As a result, the bipartite entanglement Hamiltonian defined from the MPS can be understood as a boundary conformal field theory with a physical *and* an entanglement boundary. We are able to exploit the symmetry properties of the MPS to engineer the physical conformal boundary condition. The entanglement boundary, on the other hand, is related to the concrete lattice model and remains invariant under this relevant perturbation. Using critical lattice models described by the Ising, Potts, and free compact boson conformal field theories, we illustrate the influence of the symmetry and the relevant deformation on the conformal boundaries in the entanglement spectrum.

DOI: 10.1103/PhysRevLett.132.086503

Introduction.—The past decades have witnessed the successful application of ideas from quantum information theory in quantum many-body physics, providing new insights beyond conventional many-body techniques [1]. The central insight concerns the entanglement structure in the low-energy states of correlated quantum many-body systems, summarized in the entanglement area law [2] for gapped states or the logarithmic violations thereof in critical systems [3,4]. Here the entanglement Hamiltonian H_E, also called the modular Hamiltonian, plays a pivotal role. In a given quantum many-body state, it arises when considering the reduced density matrix of a subsystem, and is defined as

$$\rho = \frac{1}{\mathcal{Z}} \exp\left(-2\pi H_E\right), \tag{1}$$

in which $\mathcal{Z}$ is a normalization factor preserving the unit trace of ρ. The low-lying spectrum of H_E or *entanglement spectrum* often contains fingerprints of the exotic nature of a given quantum state, and can be used as a diagnostic tool in numerical simulations. Famous examples are the degeneracies in the entanglement spectrum of a state with symmetry-protected topological (SPT) order in one dimension [5,6] or the universal form of the entanglement spectrum of a fractional quantum Hall state [7]. The entanglement spectrum also directly determines the entanglement entropy in a given state, which has been identified as one of the key quantities for characterizing topological order [8,9].

For *critical* phases, the formalism of conformal field theory (CFT) has revealed universal properties of entanglement spectra in one-dimensional systems [3,10,11]. It was observed that the structure of the entanglement spectrum in critical spin chains is the one of a boundary conformal field theory (BCFT) [12], an observation that was later formalized [13]. In a more recent work, the effect of introducing a finite gap by a relevant perturbation was also tackled in general terms [14].

On the other hand, the formalism of tensor networks [15] has proven very fruitful for capturing the correlations in *gapped* systems, because they naturally model the entanglement structure inherent in the low energy states in these systems. In one dimension, gapped states are described by the class of matrix product states (MPS), to the extent that all gapped phases of one-dimensional matter can be fully classified by MPS using group cohomology [5,6]. In two dimensions, nonchiral topological order can be classified through the class of projected entangled-pair states [16] and tensor network techniques provide a direct way for calculating the entanglement spectra of chiral topological states [17,18].

An injective MPS with finite bond dimension always has a finite correlation length, and can therefore never capture the critical nature of a quantum ground state directly. Instead we have to develop a scaling theory that describes the effect of this finite bond dimension, similar to the theory of finite-size scaling that is used for extracting critical data from, e.g., Monte Carlo simulations or exact diagonalizations on finite clusters. Since a tensor network effectively truncates the amount of entanglement in a quantum state, this gives rise to the theory of *finite-entanglement scaling*. The fundamental idea has always been that simulating a critical system through MPS induces a finite length scale in the system [19–21], and that this length scale can be used to perform a scaling analysis. This approach has led to a number of interesting results [22–30], making MPS methods very powerful for simulating critical phenomena. Yet, despite these successes, the effect of finite-entanglement scaling on the entanglement spectrum itself has not been addressed.

In this Letter, we use the aforementioned CFT results to shed new light on this fundamental question. We will simulate critical spin chain models with MPS in the thermodynamic limit directly, for which the only approximation is due to the finite bond dimension. We will argue that this entanglement cutoff induces a relevant perturbation of the critical system, and show that this perfectly explains the observed structure in MPS entanglement spectra. In fact, we will show that we can engineer the form of the perturbation by imposing symmetries on the MPS representation.

General framework.—Consider a critical spin chain with Hamiltonian H^*, for which the low energy properties are described by an effective CFT. We construct a variational MPS ground state approximation for a Hamiltonian in the vicinity of H^* directly in the thermodynamic limit [31,32], with a given bond dimension D. We assume we are working in the regime of finite entanglement scaling where the effective length scale of the MPS state $\xi_D \coloneqq -1/\log(|\lambda|)$ (λ is the subleading eigenvalue of the transfer matrix composed by the MPS local tensor) [15] is much larger than the lattice spacing but smaller than any other length scale (e.g., from not being exactly at criticality). We now propose that this length scale can be modeled as arising from a small relevant perturbation in the CFT. The MPS can thus be viewed as the ground state of a deformed Hamiltonian

$$H = H^* + \sum_g \xi_D^{\Delta_g - 2} O_g + \ldots, \qquad (2)$$

where the O_g are all relevant operators (operators with a scaling dimension $\Delta_g < 2$) and the dots are additional irrelevant terms. Under a renormalization group (RG) flow, the relevant operators become more and more important. It is the most relevant perturbation O_g governing the scaling properties of MPS.

The effect of this deformation on the entanglement spectrum can be inferred similarly to the discussion in Ref. [14], where the authors considered the imaginary time action of a CFT, perturbed by a primary field. In order to obtain the entanglement Hamiltonian in half-space, one needs to consider a logarithmic conformal mapping, yielding the action

$$S = S^* + \int_0^\infty dx \int_0^{2\pi} d\tau\, e^{(2-\Delta_g)(x - \log(\xi_D))} O_g + \ldots, \qquad (3)$$

where x and τ denote the Rindler space-time coordinates [14], and O_g is the relevant perturbation from Eq. (2). One can see that the conformal mapping serves the role of an RG process to the relevant deformation. Under the logarithmic mapping, the uniform O_g term becomes exponentially large away from the entanglement boundary and the dynamics is frozen except for the region $0 < x < \log(\xi_D)$. Therefore, it becomes a BCFT with one entanglement boundary B_e and one physical boundary B_p, the latter being determined by O_g. Significantly, the two boundaries possess distinct physical interpretations and origins. The physical boundary is determined by the relevant deformation in the bulk, while the entanglement one reflects the relation between different degrees of freedom. The entanglement spectrum takes the form of a BCFT spectrum,

$$\Delta_i \sim \frac{\pi}{\log(\xi_D)} (\Delta_h + n_i), \qquad (4)$$

where n_i is a non-negative integer, h is the primary that marks the conformal tower V_h determined by the fusion rule $V_e \otimes V_g \sim C_{e,g}^h V_h$ following the modular invariance of the partition function [33–37]. The distribution of Δ_i provides a clear indicator to identify the deformation O_g to the CFT [33–37].

Among all the allowed relevant deformations in Eq. (2), the entanglement truncation in MPS chooses the most relevant perturbation O_g that is allowed by the symmetries of the MPS. In generic MPS (with only translation symmetry), the perturbation imposed by the entanglement truncation should be the primary operator with the lowest conformal weight in the corresponding CFT. In continuous phase transitions with symmetry breaking, the most relevant operator is usually a symmetry-breaking term. This explains why finite entanglement tends to result in ordered MPS at the critical point. However, when we impose symmetry constraints in the MPS representation, such a field term is not allowed in Eq. (2), and another deformation will determine the scaling behavior. So we can use the symmetry constraints in the MPS as a selection rule to impose different physical conformal boundaries in the entanglement spectrum.

Physical conformal boundaries in MPS.—As a first illustration of our approach, we consider the quantum Ising chain with transverse magnetic field

$$H = -\sum_i \sigma_i^z \sigma_{i+1}^z - h \sum_i \sigma_i^x. \qquad (5)$$

It has a global $\mathbb{Z}_2$ symmetry and undergoes a continuous phase transition when tuning the field across $h = 1$. This model realizes an Ising CFT at the critical point. We use variational MPS methods [31,32] to find ground state approximations for a given bond dimension D directly in the thermodynamic limit. We can easily constrain the MPS approximation to be invariant under the $\mathbb{Z}_2$ symmetry by imposing a sparse block structure onto the MPS tensors. We can assume the entanglement boundary to be free [12], but elaborate on this in the next section.

In Fig. 1, we show the correlation length and entanglement spectra from nonsymmetric (top) and $\mathbb{Z}_2$-symmetric (bottom) MPS simulations. The phase transition is signaled by the singular behaviour of the correlation length ξ [38], where the singular point approaches the true critical point. An interesting observation is that the direction of this shift of the critical point is different in the $\mathbb{Z}_2$-symmetric and nonsymmetric cases. This indeed implies that the symmetry of the MPS representation determines the perturbation O_g, and that the scaling behavior is therefore very different in both cases.

Let us now investigate the entanglement spectra in some detail. First of all, we note that they all show the $1/\log(\xi)$ scaling behavior, in correspondence with the finite-size scaling of Ref. [12]. In the symmetry-broken case, the most relevant perturbation is a field term, which induces a fixed up $|I\rangle$ or down $|\epsilon\rangle$ physical conformal boundary B_p. Together with the free entanglement boundary B_e, the entanglement spectrum resembles the operator contents of a BCFT with mixed boundaries, following the fusion rule $\sigma \otimes I/\varepsilon = \sigma$. Here the fixed or free boundary means a boundary condition without fluctuation in the temporal or spatial direction, respectively, [33–35,39,40]. As a result, the spectrum only contains the spin operator family V_σ. In the $\mathbb{Z}_2$-symmetric MPS, the most relevant perturbation is the energy operator, leading to a free physical boundary $|\sigma\rangle$. As the entanglement boundary remains free, the entanglement spectrum follows from the fusion rule $\sigma \otimes \sigma = I + \epsilon$.

A similar analysis also applies to the critical three-state Potts model. [37,41], where we can either impose the $\mathbb{Z}_3$ symmetry or not. The result is shown in Fig. 2. One can also consider the charge conjugation symmetry in MPS, where a charge-neutral fixed physical boundary is realized [37].

Besides the minimal models, which describe symmetry breaking transitions, we also study the entanglement spectrum in the XXZ quantum spin chain,

$$H = \sum_i \sigma_i^x \sigma_{i+1}^x + \sigma_i^y \sigma_{i+1}^y + g \sigma_i^z \sigma_{i+1}^z. \qquad (6)$$

In the region $|g| < 1$, the low energy physics can be described by a $c = 1$ free compact boson CFT. When using MPS to

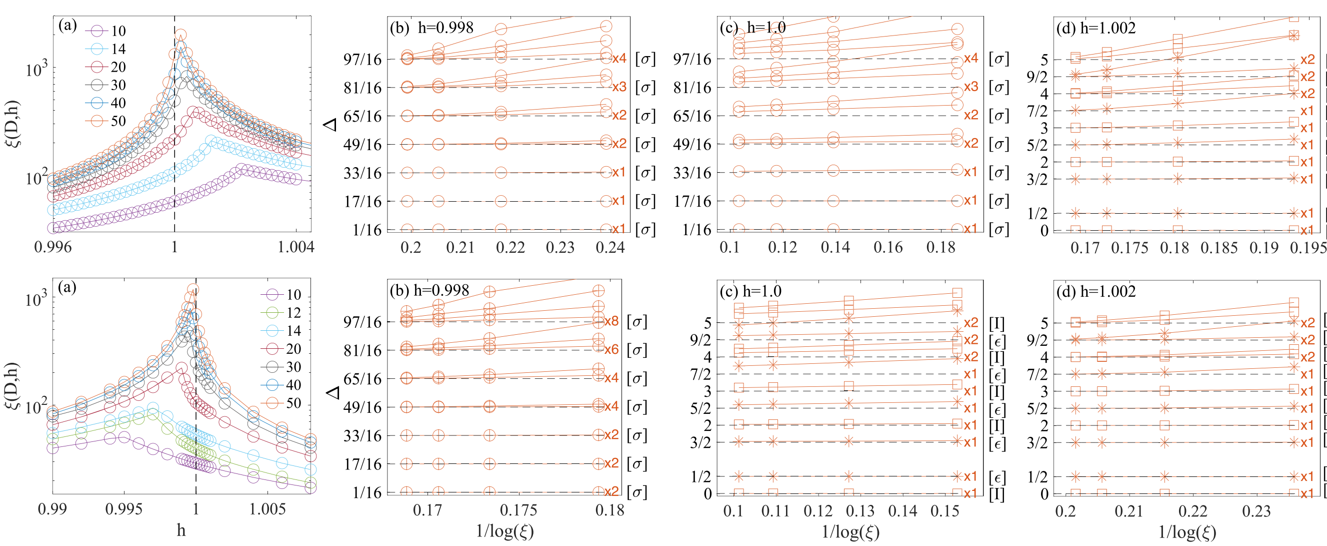

FIG. 1. Correlation length (a) and entanglement spectra (b)–(d) for the quantum Ising chain Eq. (5) obtained with non-symmetric MPS (top) and $\mathbb{Z}_2$-symmetric MPS (bottom). In (a) the dashed line denotes the critical point $h = 1$ and different curves correspond to different D as shown in the legend. In (b)–(d) the entanglement spectra have been shifted and rescaled with the first gap. σ, I, and ϵ represent the spin, identity, and energy operators, respectively. Dashed lines show the theoretical data. Here and throughout this Letter, the entanglement spectrum is rescaled according to $[(\Delta_i - \Delta_0)/(\Delta_1 - \Delta_0)]h_0$, where h_0 is the smallest gap appearing in the conformal family.

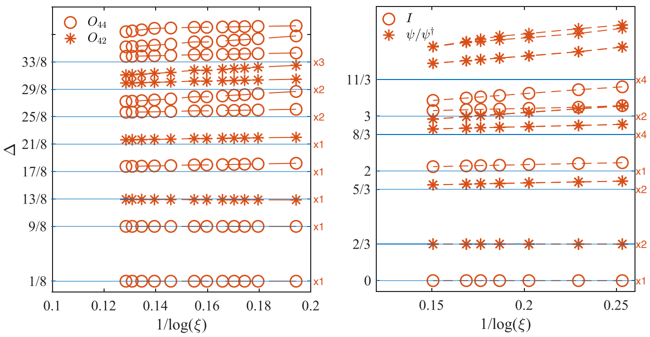

FIG. 2. Entanglement spectrum obtained from the nonsymmetric (left) and $\mathbb{Z}_3$-symmetric (right) MPS for the critical three-state Potts chain. Different markers are used to represent different conformal towers revealed by the spectrum. The spectrum has been normalized with the first energy gap. In the right panel, each $\psi/\psi^\dagger$ spectrum has a twofold degeneracy (the degeneracy in the two largest ones is slightly lifted at small length scales). O_{rs} represent primaries in the Potts CFT.

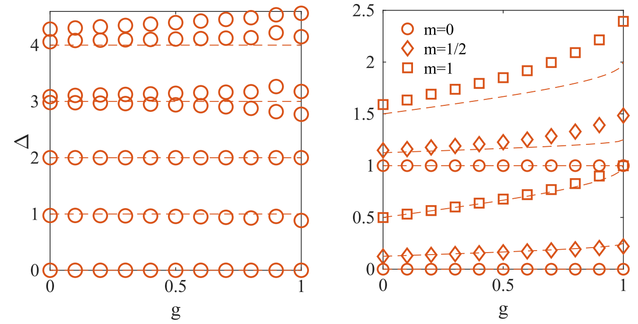

FIG. 3. Entanglement spectra for the XXZ spin chain obtained with nonsymmetric MPS (left) and $U(1)$-symmetric MPS (right). Dashed lines show the theoretical curve. In the nonsymmetric MPS simulation, we set $D = 90$. In the $U(1)$ symmetric MPS simulation, we set the truncation error to be 10^{-5}. The spectrum on the right is obtained by combining the entanglement spectra from the even and odd cuts in the two-site MPS, without making additional normalizations.

approximate its ground state, the finite entanglement cutoff tends to break either the $U(1)$ symmetry resulting in a Néel ordered state, or the translation invariance resulting in a dimerized state, as dictated by the Lieb-Schultz-Mattis theorem [42]. Again, these two cases can be understood as arising from a perturbation of the critical model, in casu, a staggered field in the xy plane or a dimerization term, respectively. The Néel ordered case is realized in the nonsymmetric MPS simulations, similar to the quantum Ising chain calculation. The dimerized state appears if we use $U(1)$ symmetric MPS with a two-site unit cell, with integer $U(1)$ charges on the odd bonds and half-integer charges on the even bonds.

From the Abelian bosonization analysis [37,43], the Néel and dimerized ordered states correspond to the Dirichlet fixed boundary and the Neumann free boundary conditions for the scalar field ϕ, respectively. To be consistent with the $U(1)$ symmetry in the state, the entanglement boundary realizes a free boundary condition for the scalar field ϕ. These boundary conditions can be verified in finite spin chains with a boundary field [37]. As a result, the entanglement spectra are very different in the two cases as shown in Fig. 3. In the Néel ordered case, the entanglement Hamiltonian realizes a mixed boundary BCFT. This case is particularly interesting since the spectrum does not depend on the radius of the compact boson or g in Eq. (6) at all. In the dimerized case, the MPS realizes a free boundary BCFT.

Entanglement conformal boundary in topological transitions.—We have shown how to control the physical boundary B_p in the MPS entanglement spectrum, but the entanglement boundary B_e was fixed by the lattice model. In order to realize nontrivial entanglement boundaries, we can look at transitions between an SPT ordered and a symmetry breaking state [44–47].

As an example, we take the cluster Ising spin chain

$$H = \sum_i -\sigma_i^z\sigma_{i+1}^z - h\left(\sigma_i^z\tau_i^x\sigma_{i+1}^z + \tau_i^z\sigma_{i+1}^x\tau_{i+1}^z\right). \quad (7)$$

This model also realizes the Ising CFT at $h = 1$ between a symmetry breaking phase and an SPT phase protected by the on-site $\mathbb{Z}_2^\sigma \times \mathbb{Z}_2^\tau$ symmetry. The new term is related to the usual transverse field term in Eq. (5) through a global unitary transformation, which can be viewed as a symmetry twist of the quantum Ising spin chain [45–47]. This twist results in a different entanglement boundary B_e [37,47].

This is confirmed by the numerical data from the MPS simulation as shown in Fig. 4, where we show the entanglement spectrum of the nonsymmetric and $\mathbb{Z}_2$-symmetric MPS at the critical point. Although the MPS share similar bulk properties with the conventional Ising transition in Fig. 1, the operator contents realized in the entanglement spectrum are very different. The physical boundary B_p is

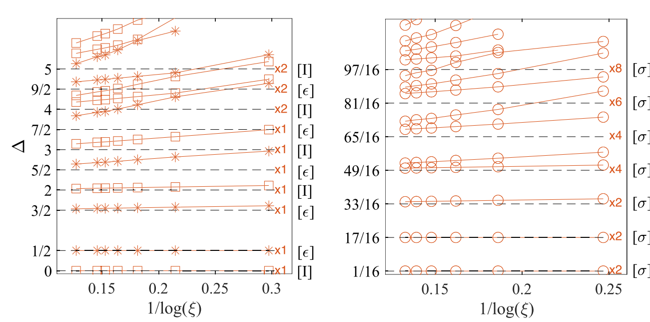

FIG. 4. Entanglement spectrum obtained from the nonsymmetric (left) and $\mathbb{Z}_2$-symmetric (right) MPS for the critical cluster Ising chain. The entanglement spectrum has been shifted and rescaled with the first energy gap. σ, I, and ϵ represent the spin, identity, and energy operators, respectively. Dashed lines show theoretical values of conformal weights.

the same as in the untwisted Ising model Eq. (5), but now the entanglement boundary B_e is a superposition of up and down fixed boundary states [45,47]. It appears that the entanglement boundary inherits the nature of the SPT phase transition, even when the bulk states are ordered. As a result, in the symmetric phase the entanglement spectrum has an exact double degeneracy for each level due to the symmetry twisted B_e [37].

Conclusions and outlook.—In this Letter we have studied the entanglement spectrum in infinite MPS from the BCFT viewpoint. The entanglement Hamiltonian can be described by a BCFT with an entanglement and physical conformal boundary at low energies. We have explicitly related the effect of an entanglement cutoff to a relevant deformation of the CFT describing the critical point. By controlling the symmetry of the MPS, we can alter this deformation and thus the physical boundary. The entanglement boundary, on the other hand, is related to the lattice model and phase transition mechanism. We expect that our Letter will prove very valuable for extracting universal scaling properties of $1+1$ dimensional quantum critical points with tensor networks.

It would be interesting to extend our insights to more general algebraic symmetries in MPS [48,49] in order to complete all physical boundary conditions. Another interesting question is to identify and classify emergent entanglement boundaries. Since the entanglement boundary remains invariant under bulk deformations, it can be used as an indicator to classify symmetry-enriched quantum critical points. It would also be interesting to study entanglement spectra in critical models without conformal symmetry [50,51]: Near a CFT, the conformal symmetry breaking term can be treated as a perturbation and the perturbative picture used here may be applied to study such theories.

Finally, our result has potential applications for studying the entanglement properties of two-dimensional quantum systems. In particular, it is expected that the boundary MPS of critical PEPS [52,53] show a similar scaling of their entanglement spectra [54]. Since the boundary MPS is known to encode the entanglement Hamiltonian of the PEPS [17], we can expect that this scaling carries important information on the topological features of the PEPS itself [37]. Also, our results suggest that the finite correlation length scaling in PEPS approximations for two-dimensional quantum critical points [27–29] can also be understood in terms of perturbed 3D CFT; in particular, we can generalize our framework for engineering the different perturbations arising from imposing symmetry constraints in PEPS.

We would like to thank Shenghan Jiang, Luca Tagliacozzo, Lars Bonnes, Huajia Wang, Laurens Lootens, Maarten Van Damme, and Tao Xiang for many helpful discussions. This work was supported by the Research Foundation Flanders, Grants No. G0E1820 and No. G0E1520N. R. Z. H. is supported by a postdoctoral fellowship from the Special Research Fund (BOF) of Ghent University. L. Z. is supported by the National Natural Science Foundation of China (No. 12174387), and the Innovative Program for Quantum Science and Technology (No. 2021ZD0302600). L. V. is supported by the Research Foundation Flanders (FWO20/PDS/11).

*ruizhen.huang@ugent.be

[1] B. Zeng, X. Chen, D.-L. Zhou, and X.-G. Wen, *Quantum Information Meets Quantum Matter* (Springer, New York, 2019).
[2] J. Eisert, M. Cramer, and M. B. Plenio, Colloquium: Area laws for the entanglement entropy, Rev. Mod. Phys. **82**, 277 (2010).
[3] G. Vidal, J. I. Latorre, E. Rico, and A. Kitaev, Entanglement in quantum critical phenomena, Phys. Rev. Lett. **90**, 227902 (2003).
[4] M. M. Wolf, Violation of the entropic area law for fermions, Phys. Rev. Lett. **96**, 010404 (2006).
[5] F. Pollmann, A. M. Turner, E. Berg, and M. Oshikawa, Entanglement spectrum of a topological phase in one dimension, Phys. Rev. B **81**, 064439 (2010).
[6] X. Chen, Z.-C. Gu, and X.-G. Wen, Classification of gapped symmetric phases in one-dimensional spin systems, Phys. Rev. B **83**, 035107 (2011).
[7] H. Li and F. D. M. Haldane, Entanglement spectrum as a generalization of entanglement entropy: Identification of topological order in non-Abelian fractional quantum Hall effect states, Phys. Rev. Lett. **101**, 010504 (2008).
[8] A. Kitaev and J. Preskill, Topological entanglement entropy, Phys. Rev. Lett. **96**, 110404 (2006).
[9] M. Levin and X.-G. Wen, Detecting topological order in a ground state wave function, Phys. Rev. Lett. **96**, 110405 (2006).
[10] P. Calabrese and J. L. Cardy, Entanglement entropy and quantum field theory, J. Stat. Mech. (2004) P06002.
[11] P. Calabrese and A. Lefevre, Entanglement spectrum in one-dimensional systems, Phys. Rev. A **78**, 032329 (2008).
[12] A. M. Läuchli, Operator content of real-space entanglement spectra at conformal critical points, arXiv:1303.0741.
[13] J. L. Cardy and E. Tonni, Entanglement Hamiltonians in two-dimensional conformal field theory, J. Stat. Mech. (2016) 123103.
[14] G. Y. Cho, A. W. W. Ludwig, and S. Ryu, Universal entanglement spectra of gapped one-dimensional field theories, Phys. Rev. B **95**, 115122 (2017).
[15] J. I. Cirac, D. Pérez-García, N. Schuch, and F. Verstraete, Matrix product states and projected entangled pair states: Concepts, symmetries, theorems, Rev. Mod. Phys. **93**, 045003 (2021).
[16] N. Schuch, J. I. Cirac, and D. Pérez-García, PEPS as ground states: Degeneracy and topology, Ann. Phys. (Amsterdam) **325**, 2153 (2010).
[17] J. I. Cirac, D. Poilblanc, N. Schuch, and F. Verstraete, Entanglement spectrum and boundary theories with projected entangled-pair states, Phys. Rev. B **83**, 245134 (2011).
[18] D. Poilblanc, J. I. Cirac, and N. Schuch, Chiral topological spin liquids with projected entangled pair states, Phys. Rev. B **91**, 224431 (2015).

[19] T. Nishino, K. Okunishi, and M. Kikuchi, Numerical renormalization group at criticality, Phys. Lett. A **213**, 69 (1996).

[20] L. Tagliacozzo, T. R. de Oliveira, S. Iblisdir, and J. I. Latorre, Scaling of entanglement support for matrix product states, Phys. Rev. B **78**, 024410 (2008).

[21] F. Pollmann, S. Mukerjee, A. M. Turner, and J. E. Moore, Theory of finite-entanglement scaling at one-dimensional quantum critical points, Phys. Rev. Lett. **102**, 255701 (2009).

[22] B. Pirvu, G. Vidal, F. Verstraete, and L. Tagliacozzo, Matrix product states for critical spin chains: Finite-size versus finite-entanglement scaling, Phys. Rev. B **86**, 075117 (2012).

[23] V. Stojevic, J. Haegeman, I. P. McCulloch, L. Tagliacozzo, and F. Verstraete, Conformal data from finite entanglement scaling, Phys. Rev. B **91**, 035120 (2015).

[24] E. Tirrito, N. J. Robinson, M. Lewenstein, S.-J. Ran, and L. Tagliacozzo, Characterizing the quantum field theory vacuum using temporal matrix product states, arXiv:1810.08050.

[25] J. C. Pillay and I. P. McCulloch, Cumulants and scaling functions of infinite matrix product states, Phys. Rev. B **100**, 235140 (2019).

[26] M. M. Rams, P. Czarnik, and L. Cincio, Precise extrapolation of the correlation function asymptotics in uniform tensor network states with application to the Bose-Hubbard and XXZ models, Phys. Rev. X **8**, 041033 (2018).

[27] M. Rader and A. M. Läuchli, Finite correlation length scaling in Lorentz-invariant gapless iPEPS wave functions, Phys. Rev. X **8**, 031030 (2018).

[28] P. Corboz, P. Czarnik, G. Kapteijns, and L. Tagliacozzo, Finite correlation length scaling with infinite projected entangled-pair states, Phys. Rev. X **8**, 031031 (2018).

[29] B. Vanhecke, J. Haegeman, K. Van Acoleyen, L. Vanderstraeten, and F. Verstraete, Scaling hypothesis for matrix product states, Phys. Rev. Lett. **123**, 250604 (2019).

[30] A. A. Eberharter, L. Vanderstraeten, F. Verstraete, and A. M. Läuchli, Extracting the speed of light from matrix product states, Phys. Rev. Lett. **131**, 226502 (2023).

[31] V. Zauner-Stauber, L. Vanderstraeten, M. T. Fishman, F. Verstraete, and J. Haegeman, Variational optimization algorithms for uniform matrix product states, Phys. Rev. B **97**, 045145 (2018).

[32] L. Vanderstraeten, J. Haegeman, and F. Verstraete, Tangent-space methods for uniform matrix product states, SciPost Phys. Lect. Notes 7 (2019).10.21468/SciPostPhysLectNotes.7

[33] J. L. Cardy, Conformal invariance and surface critical behavior, Nucl. Phys. **B240**, 514 (1984).

[34] J. L. Cardy, Effect of boundary conditions on the operator content of two-dimensional conformally invariant theories, Nucl. Phys. **B275**, 200 (1986).

[35] J. L. Cardy, Boundary conditions, fusion rules and the verlinde formula, Nucl. Phys. **B324**, 581 (1989).

[36] N. Andrei *et al.*, Boundary and defect CFT: Open problems and applications, J. Phys. A **53**, 453002 (2020).

[37] See Supplemental Material at http://link.aps.org/supplemental/10.1103/PhysRevLett.132.086503 for more discussions about BCFT, entanglement spectrum in Potts chain and XXZ Heisenberg spin chain.

[38] C. Liu, L. Wang, A. W. Sandvik, Y.-C. Su, and Y.-J. Kao, Symmetry breaking and criticality in tensor-product states, Phys. Rev. B **82**, 060410(R) (2010).

[39] J. L. Cardy, Bulk renormalization group flows and boundary states in conformal field theories, SciPost Phys. **3**, 011 (2017).

[40] R. Blumenhagen and E. Plauschinn, *Introduction to Conformal Field Theory: With Applications to String Theory* (Springer Berlin, Heidelberg, 2009), Vol. 779.

[41] I. Affleck, M. Oshikawa, and H. Saleur, Boundary critical phenomena in the three-state Potts model, J. Phys. A **31**, 5827 (1998).

[42] E. Lieb, T. Schultz, and D. Mattis, Two soluble models of an antiferromagnetic chain, Ann. Phys. (N.Y.) **16**, 407 (1961).

[43] T. Giamarchi, *Quantum Physics in One Dimension*, Vol. 121 (Clarendon Press, Oxford, 2003).

[44] G. Y. Cho, K. Shiozaki, S. Ryu, and A. W. W. Ludwig, Relationship between symmetry protected topological phases and boundary conformal field theories via the entanglement spectrum, J. Phys. A **50**, 304002 (2017).

[45] T. Scaffidi, D. E. Parker, and R. Vasseur, Gapless symmetry-protected topological order, Phys. Rev. X **7**, 041048 (2017).

[46] R. Verresen, R. Thorngren, N. G. Jones, and F. Pollmann, Gapless topological phases and symmetry-enriched quantum criticality, Phys. Rev. X **11**, 041059 (2021).

[47] X.-J. Yu, R.-Z. Huang, H.-H. Song, L. Xu, C. Ding, and L. Zhang, Conformal boundary conditions of symmetry-enriched quantum critical spin chains, Phys. Rev. Lett. **129**, 210601 (2022).

[48] L. Lootens, J. Fuchs, J. Haegeman, C. Schweigert, and F. Verstraete, Matrix product operator symmetries and intertwiners in string-nets with domain walls, SciPost Phys. **10**, 053 (2021).

[49] J. Garre-Rubio, L. Lootens, and A. Molnár, Classifying phases protected by matrix product operator symmetries using matrix product states, Quantum **7**, 927 (2023).

[50] J. L. Cardy, Critical exponents of the chiral Potts model from conformal field theory, Nucl. Phys. **B389**, 577 (1993).

[51] S. Whitsitt, R. Samajdar, and S. Sachdev, Quantum field theory for the chiral clock transition in one spatial dimension, Phys. Rev. B **98**, 205118 (2018).

[52] S.-J. Ran, C. Peng, W. Li, M. Lewenstein, and G. Su, Criticality in two-dimensional quantum systems: Tensor network approach, Phys. Rev. B **95**, 155114 (2017).

[53] H. Dreyer, L. Vanderstraeten, J.-Y. Chen, R. Verresen, and N. Schuch, Robustness of critical U(1) spin liquids and emergent symmetries in tensor networks, arXiv:2008.04833.

[54] As an illustrative example, see the Supplemental Material at [37] for the case of the nearest-neighbor RVB, which includes Refs. [55–57].

[55] E. Ardonne, P. Fendley, and E. Fradkin, Topological order and conformal quantum critical points, Ann. Phys. (Amsterdam) **310**, 493 (2004).

[56] P. W. Anderson, The resonating valence bond state in La_2CuO_4 and superconductivity, Science **235**, 1196 (1987).

[57] F. Verstraete, M. M. Wolf, D. Pérez-García, and J. I. Cirac, Criticality, the area law, and the computational power of projected entangled pair states, Phys. Rev. Lett. **96**, 220601 (2006).